

Modelling and verification of melanin concentration on human skin type

| | |
|-------------------------------|---|
| Journal: | <i>Photochemistry and Photobiology</i> |
| Manuscript ID: | Draft |
| Wiley - Manuscript type: | Research Article |
| Date Submitted by the Author: | n/a |
| Complete List of Authors: | Karsten, Aletta; CSIR, National Laser Centre Smit, Jacoba; CSIR, Biosciences |
| Keywords: | Computer simulation, melanin concentration, skin-like phantoms, epidermal thickness, absorption spectra |
| | |

1 **Modelling and verification of melanin concentration on human skin type**

2 Mrs Aletta E Karsten^{1,2}, Dr Jacoba E Smit^{*,3,4}

3 ¹Biophotonics group, National Laser Centre, CSIR, PO Box 395, Pretoria, 0001, South Africa

4 ²Department of Physics, University of Pretoria, Pretoria, 0002, South Africa

5 ³Biosciences, CSIR, PO Box 395, Pretoria, 0001, South Africa

6 ⁴Modelling and Digital Sciences, CSIR, PO Box 395, Pretoria, 0001, South Africa

7

8 * Corresponding author's name and email: Jacoba E Smit (KSmit@csir.co.za)

* To whom correspondence should be addressed, at Modelling and Digital Sciences, CSIR, PO Box 395, Pretoria, 0001, South Africa; fax: + 27 12 841 2456; email: KSmit@csir.co.za;

For Peer Review

1

2 **ABSTRACT**

3

4 Lasers are used in the minimalistic or non-invasive diagnosis and treatment of skin disorders.
5 Less laser light reaches the deeper skin layers in dark skin types, due to its higher epidermal
6 melanin concentration compared to lighter skin. Laser-tissue interaction modelling software
7 can correct for this by adapting the dose applied to the skin. This necessitates an easy and
8 reliable method to determine the skin's type. Non-invasive measurement of the skin's
9 melanin content is the best method. However, access to samples of all skin types is often
10 limited and skin-like phantoms are used instead. This study's objective is to compare
11 experimentally measured absorption features of liquid skin-like phantoms representing Skin
12 Types I to VI with a realistic skin computational model component of ASAP®. Sample UV-
13 VIS transmittance spectra were measured from 370 to 900 nm and compared to simulated
14 results from ASAP® using the same optical parameters. Results indicated non-monotonic
15 absorption features towards shorter wavelengths, which may allow for more accurate ways of
16 determining melanin concentration and expected absorption through the epidermal layer. This
17 suggests possible use in representing optical characteristics of real skin. However, a more
18 comprehensive model and phantoms are necessary to account for the effects of sun exposure.

19

1

2 **INTRODUCTION**

3

4 In the past 50 years lasers have found numerous applications in medicine, both for treatment
5 and diagnostics (1). One of the advantages of lasers is that they can be used for minimalistic
6 or non-invasive diagnosis and treatment. Often that means that the light must penetrate
7 through the skin and the correct dose required, relies on accurate information regarding the
8 skin's optical properties (2).

9 Human skin consists of different layers, with the epidermal layer containing the
10 melanin that is responsible for skin tone or skin type (3). Epidermal melanin can broadly be
11 divided into two types, eumelanin (black-brown colour) and pheomelanin (yellow-reddish
12 colour) (3,4). Melanin is synthesized within melanosomes inside melanocytes located in the
13 basal layer of the epidermis and the mature melanosomes get transferred via dendrites to the
14 keratinocytes in die epidermis where they are responsible for skin photoprotection (3).

15 It is well documented that the absorption and scattering of light through skin tissue
16 depends on the skin's optical properties (see for example studies by Tuchin (5)). Melanin
17 absorbs light in the visible and near infrared parts of the spectrum, the part most suitable for
18 diagnostics and treatment due to deeper penetration (1). Absorption of light in the epidermal
19 layer is a major factor in determining the fluence of the laser light that reaches the deeper
20 levels of the skin. Darker skin has an epidermal melanin volume fraction of about twice that
21 of lighter skins (6). Due to melanin absorption, less laser light reaches the deeper parts of the
22 skin in dark skin types (1). This can be corrected for by laser-tissue interaction modelling
23 software to adapt the dose applied to the skin. In order to correctly apply such software it is
24 important to characterise the skin in terms of skin type with an easy and reliable method.

1 Measuring the melanin content of the skin is the best method, but it needs to be done
2 non-invasively. In a recent review Brenner and Hearing (7) discussed the photoprotective role
3 and physiologic changes of melanin when human skin, covering the different Fitzpatrick Skin
4 Types I to VI (8), is irradiated with ultra-violet (UV) light. Studies covered in the review
5 where performed *in vivo* and/or *in vitro* and elucidated the melanosomal differences between
6 the different skin types. Meinhardt et al (9) measured the absorption spectra of *in vivo* human
7 skin from the lighter skin types before and after exposure to natural UV radiation, while Wan
8 et al (10) measured the epidermal (including the Stratum corneum) transmittance of *in vitro*
9 light and dark coloured human skin over the UVA, UVB and visible wavelength ranges.
10 None of these studies however specifically determined epidermal melanin concentration in
11 the different skin types. The absorption features of melanin is monotone in the visible and
12 near infra-red parts of the spectrum (11), but over UV wavelengths melanin absorption
13 display non-monotonic features (9) that may allow for more accurate ways of determining
14 melanin concentration and therefore the expected absorption through the epidermal layer.

15 Human skin of the different Skin Types I to VI is not always readily available. Hence
16 the use of skin-like phantoms (12). Previous results with skin-like phantoms representing
17 Skin Types I to VI indicated the possibility of predicting some of the non-monotonic optical
18 characteristics of real human skin, albeit in the visible wavelength range as opposed to the
19 UV range in real human skin (13). The purpose of this study is to compare the experimentally
20 measured absorption features of these liquid skin-like phantoms with computational
21 simulated skin from the Realistic Skin Model (RSM) part of the Advanced Systems Analyses
22 Program (ASAP®) software from Breault Research. It forms the first phase of the larger
23 objective of knowledge acquisition about the optical properties of real human skin cell tissue
24 to enhance the accuracy of these computational simulated skin models.

25

1 MATERIALS AND METHODS

2

3 *Computer simulations.* The ASAP® commercial software from Breault Research is
4 fundamentally a flexible and efficient optical system raytracing modelling tool, allowing
5 users to easily make geometry changes to a tissue model. The ray tracing is based on the
6 Monte Carlo ray tracing techniques, where “photons” or “rays” are traced through an optical
7 medium with pre-defined absorption and scattering properties. The rays can automatically
8 split into reflected, refracted, diffracted, polarized and scattered components as they
9 propagate through the system. Each of the rays proceeds independently, interacting with the
10 encountered optical surfaces in any order, as appropriate. This type of ray tracing is often
11 described as “non-sequential” ray tracing. It is a simulation, based on the way that real light
12 waves behave in the real world.

13 The Realistic Skin Model (RSM) part of the ASAP® software from Breault Research,
14 was used as the modeling tool for this work. The skin model consisted of four layers, the
15 Stratum corneum (SC), the epidermis (containing the melanosomes, the main absorbing
16 particles), the dermis and the hypodermis. The hypodermis was not taken into account in this
17 study. A graphical layout of the model is shown in Figure 1. The optical properties for the
18 different layers in the model are reported in Tables 1 and 2.

19 > *Figure 1* <

20 Different skin types were simulated by changing the volume fraction of the
21 melanosomes in the epidermis (14) as indicated in Table 1. The variation used corresponds to
22 published data that reported a more than 10 fold increase in the absorption coefficient (from
23 0.2 mm^{-1} to 2.5 mm^{-1}) between Caucasian and African skin at 694 nm (15,16). In humans, the

1 thickness of the epidermis varies from 38 μm in the cheek to 369 μm on the finger tip (17).
2 Two different sun exposed skin areas were evaluated in this work, the cheek (epidermal
3 thickness of 38 μm) and the back of the hand (87.5 μm). A Gaussian laser beam (power
4 10 mW) with a beam waist of 0.4 mm was used as the light source in the model. Wavelengths
5 between 300 and 1000 nm were used in this work. The shorter wavelengths were used due to
6 the absorption features of melanin in the UV part of the spectrum and the other wavelengths
7 selected are wavelengths that are applicable in laser treatments. The four important optical
8 parameters that influence the propagation of light through tissue are the absorption coefficient
9 (μ_a), the scattering coefficient (μ_s), the anisotropy factor (g) and the refractive index (n) (18).
10 For this study published data of the optical parameters were used (14,17,19). The values of μ_a
11 and μ_s are determined by the concentrations of the absorbing and scattering particles in the
12 different skin layers. The thickness of the different layers (d), g and n are listed in Table 2.
13 The surface of the model is 10 mm² and the depth (Z dimension) varies from 1.853 to
14 1.9025 mm, depending on the epidermal thickness. The values of both n and g (2) were kept
15 the same over the wavelength range. In the model the optical properties for each layer are
16 specified separately, but assumed uniform throughout a specific layer. Each photon is tracked
17 until it is either absorbed in the model or exits the boundaries of the model. The skin model
18 was divided into 150 layers and each layer into 150x150 segments to form small 3-
19 dimensional volumes or voxels. The photons absorbed in each of the voxels were registered
20 to give the total absorption in each layer.

21

22 *Liquid melanin skin-like phantoms: Sample preparation.* Melanin samples at concentrations
23 ranging from 0.011 mg/mL to 1.3 mg/mL were prepared from a eumelanin (Sigma-Aldrich
24 M0418) stock solution at physiological pH (~7.01) as previously described in Smit et al. (13).
25 Skin-like phantoms were prepared by adding either 3 μL or 30 μL Intralipid (IL) (Sigma-

1 Aldrich I141) to 3 mL of each of the melanin samples. Intralipid is a phospholipid-stabilized
2 soybean oil, supplied as 20% fat emulsion.

3

4 *Liquid melanin skin-like phantoms: Sample preparation.* A UV-VIS spectrophotometer
5 (Shimadzu UV-1650 PC) using standard 1 cm pathlength cuvettes over the wavelength range
6 370 to 900 nm was used to measure sample absorbance spectra. Total attenuation coefficients
7 ($\mu_t(\lambda)$) for the skin-like phantoms were calculated from these. The total attenuation
8 coefficient ($\mu_t(\lambda)$) is the decrease in the light intensity through the sample and is equal to
9 the combination of the absorption and scattering coefficients of the sample (5). It was
10 calculated from

$$11 \quad \mu_t(\lambda) = \frac{-\ln T(\lambda)}{L} \quad [1/cm] \quad (1.1)$$

12 with $T(\lambda)$ the wavelength dependent transmittance and L the optical pathlength (in cm).

13

14

15 RESULTS

16 UV-VIS absorbance spectra over the wavelength range 370 to 900 nm of melanin only
17 samples were measured before addition of the Intralipid (IL). Attenuation coefficients
18 ($\mu_t(\lambda)$) were calculated from these spectra and the resultant spectra showed broadband
19 attenuation without any chromophoric peaks (Fig. 2 and (13)), in accordance with trends
20 observed for synthetic melanin (12).

21 > Figure 2 <

1 Liquid skin-like phantoms were prepared by adding either 3 μL or 30 μL IL to the
2 melanin samples respectively (Figs. 3(a) and (b)). The skin-like phantoms represented fair
3 (0.011 mg/mL melanin), medium (0.066 mg/mL melanin) and dark (0.13 mg/mL melanin)
4 skin phototypes. Medium to dark phantoms displayed non-monotonic trends towards shorter
5 wavelengths. The peaks became more pronounced and shifted towards longer wavelengths as
6 the melanin concentration was increased.

7 > *Figure 3* <

8 Increasing the amount of added IL (representing a thicker epidermal layer) led to
9 increased attenuation in fairer phantoms; which was not observable in darker phantoms. The
10 non-monotonic peaks were also broadened compared to peaks from spectra representing a
11 thinner epidermal layer (compare Fig. 3(b) to 3(a)). A more detailed discussion on the skin-
12 like phantoms can be found in Smit et al (13).

13 > *Figure 4* <

14 The cumulative power absorbed by two different thicknesses of modelled human skin
15 was calculated from simulations performed with the Realistic Skin Model (RSM) part of the
16 ASAP® software for a skin depth up to 0.12 mm (Figs. 4(a) and (b)). Spectra displayed
17 similar non-monotonic trends towards shorter wavelengths as spectra of the measured skin-
18 like phantoms in Fig. 3, although more pronounced for fairer skin types in the former
19 compared to the latter. Modelled fairer skin types predicted higher absorption of incoming
20 light relative to darker skin types compared to similar spectra for the skin-like phantoms,
21 irrespective of epidermal thickness (ET). Peaks also tended to shift towards longer
22 wavelengths as modelled skin darkness increased, but were much broader than peaks for the
23 skin-like phantoms.

1

2 **DISCUSSION**

3

4 In this study the absorption features of liquid skin-like phantoms were measured over the
5 wavelength range 370 – 900 nm (UVA and VIS) and compared to modelled skin simulated
6 with the RSM part of the ASAP® software. The skin-like phantoms contained different
7 concentrations of melanin and either 3 μL or 30 μL IL were added to the samples to represent
8 thinner and thicker skin. Modelled skin represented fair, medium and dark skin types of two
9 different epidermal thicknesses (ET = 38 μm and 87.5 μm respectively).

10 Skin type (phototype) is determined by a combination of melanin and haemoglobin,
11 together with other pigments including bilirubin and carotene. Epidermal melanin can
12 broadly be divided into two types, eumelanin (black-brown colour) and pheomelanin (yellow-
13 reddish colour) (3,4). Haemoglobin dominates the absorption properties of the dermis
14 (20,21). Although different studies differ on the ratios of pheomelanin to eumelanin
15 concentration between the different skin types, in general it is agreed that lighter skin types
16 contains a higher concentration pheomelanin compared to eumelanin that the darker skin
17 types (22,23). In the RSM part of the ASAP® software the default parameters for the
18 eumelanin and pheomelanin concentrations in the epidermis are 80 g/L and 12 g/L
19 respectively. The eumelanin and pheomelanin concentrations were kept at default values for
20 all skin types, while the value for the volume fraction of the melanosomes was varied (Table
21 1). The software multiplies the values of the melanin and the volume fractions to calculate the
22 amount of melanin in the epidermis. The ratio of the default values in the RSM model
23 seemed to better reflect ratios in the dark skin types than the fairer skin types. This could

1 have contributed towards the overestimation in the calculated absorption for the fairer skin
2 types.

3 The melanocytes containing the melanosomes responsible for the biosynthesis and
4 storing of the melanin are located in the basal layer of the epidermis (3,24). In reviews on
5 skin of colour, Taylor (25) and Brenner and Hearing (7) referred to studies that established
6 that the number of melanocytes is racial independent, i.e. skin type independent. It may differ
7 between individuals of the same skin type and even from one anatomical region to the next in
8 the same individual. Differences in skin type are dependent on variations in the size, number
9 and aggregation of the melanosomes, both inside the melanocytes and keratinocytes, as well
10 as on the distribution throughout the epidermis and Stratum corneum (7,25 and references
11 therein). For instance, Toda et al (26) and Olson et al (27) demonstrated differences in
12 melanosome aggregation and size between dark skinned and light skinned individuals.
13 Eumelanin is associated with larger elliptical melanosomes, while pheomelanin is associated
14 with smaller spherical melanosomes. Melanosomes are also more evenly distributed
15 throughout the epidermis and Stratum corneum in the darker skin types compared to fairer,
16 unexposed skin types where the melanosomes are observed to cluster more in the basal part
17 of the epidermis (25 and references therein). In the RSM software size and aggregation
18 parameters are not taken into account; the melanosome contribution is only represented as a
19 volume fraction. The lack of size and aggregation representation in the model could possibly
20 lead to an over- or underestimation of the melanin concentration for a specific skin type.
21 Furthermore, each of the skin layers in the model is assumed a homogeneous medium. The
22 melanin would therefore be considered evenly distributed throughout the epidermis, which
23 favours the representation of the darker skin types more compared to the fairer skin types.
24 These differences may hence partially lead to a possible overestimation in absorption
25 calculated for the fairer skin types compared to real human skin.

1 The addition of IL to the liquid melanin only samples resulted in skin-like phantoms
2 that displayed the non-monotonic absorption features observed in real human skin, albeit
3 more towards the visible than the observed UVA / UVB wavelength range in real skin.
4 Compare the results from this study for example to Meinhardt et al (9) and Wan et al (10).
5 The non-monotonic absorption features in the RSM model were similar to those of the skin-
6 like phantoms. This confirmed that the observed spectral response was indicative of the
7 melanin's immediate reaction to the absorbed light, since it is not possible with either the
8 skin-like phantoms or the RSM model to model the long term effects of induced erythema as
9 observed in the Meinhardt et al (9) and Wan et al (10) studies. Erythema induced by exposure
10 to wavelengths in the UV region shows three distinct pigmentary responses, namely
11 immediate pigment darkening (IPD), persistent pigment darkening (PPD) and delayed
12 tanning response (DTR) (7). IPD occurs immediately after sun exposure and shows a broad
13 peak in the UVA (320 – 400 nm) and visible wavelength regions (28,29). PPD occurs a few
14 hours after UV exposure and lasts a few days, while DTR appears 2-3 days after UV
15 exposure, is induced by either UVA or UVB and lasts for about 3-4 weeks (7 and references
16 therein). In the Meinhardt et al (9) study the subjects were re-evaluated after two weeks' sun
17 exposure with absorbance spectra therefore exhibiting the characteristics of DTR with peaks
18 in the UVB region. The RSM model simulations and skin-like phantoms showed absorbance
19 peaks in the UVA and visible regions and could hence represent IPD. Toda et al (26), Olson
20 et al (27) and Lavker and Kaidbey (30) also demonstrated differences in melanosome
21 aggregation between sun exposed and non-exposed anatomical regions in the same
22 individuals, highlighting the effect of sun exposure. These important effects of sun exposure
23 could not be modeled with either the RSM model or skin-like phantoms, highlighting the
24 need for a model and skin-like phantoms that can be used to study the effects of sun
25 exposure.

1 In a previous paper we attributed the appearance of the non-monotonic features in the
2 skin-like phantoms to the interaction between the melanin and the IL, which differed
3 depending on the melanin concentration (13). IL is a phospholipid-stabilized soybean oil
4 consisting of an emulsion of bilipid membrane fragments of various sizes, suspended in
5 water. It is commonly used to mimic the scattering properties of human skin. Melanin is a
6 family of polymorphous multifunctional biopolymers that readily binds to cations, anions,
7 drugs and chemicals (3). Our previous results indicated that the melanin binds to the IL
8 fragments, although we do not know the exact nature of this interaction. The melanin sub-
9 complexes also tended to aggregate into increasingly larger particles as the concentration was
10 increased and we argued the possibility that such larger aggregates may bind to lipid
11 structures more readily than the smaller melanin particles associated with lower melanin
12 concentrations. Our results may therefore be interpreted that “photo-protection in darker skin
13 phototypes may not be only a function of epidermal melanin concentration, but that the
14 interaction between the melanin complex and the lipid membranes found in the skin cells
15 may play an equally important role” (13).

16 In conclusion results from both the RSM model and the liquid skin-like phantoms
17 indicated that they can be used to study the immediate effects of sun exposure of the UV and
18 visible wavelength ranges and hence the dosages required for laser based treatment of skin
19 disorders. However, more comprehensive models and phantoms are necessary to predict the
20 change in dosage required for sun exposure skin of all skin types.

21

22 *Acknowledgements*— This work was supported by CSIR Parliamentary Grants. We thank Dr
23 Raymond Sparrow and the Synthetic Biology ERA at CSIR Biosciences for use of their
24 laboratory and equipment.

25

1 **REFERENCES**

- 2
- 3 1. Peng, Q., A. Juzeniene, J. Chen, L. O. Svaasand, T. Warloe, K. E. Giercksky, and J.
- 4 Moan (2008) Lasers in medicine. *Reports on Progress in Physics* **71**, 056701-1-056701-
- 5 28.
- 6 2. Wilson, B. C. and S. L. Jacques (1990) Optical reflectance and transmittance of tissues:
- 7 Principles and applications. *IEEE J. Quantum Electron.* **26**, 2186-2199.
- 8 3. Costin, G. E. and V. J. Hearing (2007) Human skin pigmentation: Melanocytes
- 9 modulate skin color in response to stress. *FASEB J.* **21**, 976-994.
- 10 4. Liu, Y., L. Hong, K. Wakamatsu, S. Ito, B. Adhyaru, C. Y. Cheng, C. R. Bowers, and J.
- 11 D. Simon (2005) Comparison of structural and chemical properties of black and red
- 12 human hair melanosomes. *Photochem. Photobiol.* **81**, 135-144.
- 13 5. Tuchin, V. V. (2007) *Tissue Optics: Light Scattering Methods and Instruments for*
- 14 *Medical Diagnostics*. SPIE Press, Bellingham, Washington, USA.
- 15 6. Alaluf, S., S. Alaluf, A. Heath, N. I. K. Carter, D. Atkins, H. Mahalingam, K. Barrett,
- 16 R. I. A. Kolb, and N. Smit (2001) Variation in melanin content and composition in type
- 17 V and VI photoexposed and photoprotected human skin: The dominant role of DHI.
- 18 *Pigment Cell Res.* **14**, 337-347.
- 19 7. Brenner, M. and V. J. Hearing (2008) The protective role of melanin against UV
- 20 damage in human skin. *Photochem. Photobiol.* **84**, 539-549.
- 21 8. Fitzpatrick, T. B. (1988) The validity and practicality of sun-reactive skin types I
- 22 through VI. *Arch. Dermatol.* **124**, 869-871.

- 1 9. Meinhardt, M., R. Krebs, A. Anders, U. Heinrich, and H. Tronnier (2009) Absorption
2 spectra of human skin in vivo in the ultraviolet wavelength range measured by
3 optoacoustics. *Photochem. Photobiol.* **85**, 70-77.
- 4 10. Wan, S., R. R. Anderson, and J. A. Parrish (1981) Analytical modeling for the optical
5 properties of the skin with in vitro and in vivo applications. *Photochem. Photobiol.* **34**,
6 493-499.
- 7 11. Dam, J. S. (2001) Optical analysis of biological media - continuous wave techniques.
8 PhD Thesis, Lund Institute of Technology.
- 9 12. Bashkatov, A. N., E. A. Genina, V. I. Kochubey, M. M. Stolnitz, T. A. Bashkatova, O.
10 V. Novikova, A. Y. Peshkova, and V. V. Tuchin (2000) Optical properties of melanin in
11 the skin and skin-like phantoms. In Proceedings of SPIE - The International Society for
12 Optical Engineering, Vol. 4162, (Edited by Tuchin, V. V.), pp. 219-226. SPIE - The
13 International Society for Optical Engineering, Controlling Tissue Optical Properties:
14 Applications in Clinical Study, Amsterdam, Netherlands, 4 July 2000.
- 15 13. Smit, J. E., A. F. Grobler, and R. W. Sparrow (2011) Influence of variation in
16 eumelanin content on absorbance spectra of liquid skin-like phantoms. *Photochem.*
17 *Photobiol.* **87**, 64-71.
- 18 14. Jacques, S. L. and D. J. McAuliffe (1991) The melanosome: threshold temperature for
19 explosive vaporization and internal absorption coefficient during pulsed laser
20 irradiation. *Photochem. Photobiol.* **53**, 769-775.
- 21 15. Zhang, R., W. Verkruyse, B. Choi, J. A. Viator, B. Jung, L. O. Svaasand, G. Aguilar,
22 and J. S. Nelson (2005) Determination of human skin optical properties from

- 1 spectrophotometric measurements based on optimization by genetic algorithms. *J.*
2 *Biomed. Opt.* **10**, 1-11.
- 3 16. Zonios, G., J. Bykowski, and N. Kollias (2001) Skin melanin, hemoglobin, and light
4 scattering properties can be quantitatively assessed in vivo using diffuse reflectance
5 spectroscopy. *J. Invest. Dermatol.* **117**, 1452-1457.
- 6 17. Whitton, J. T. and J. D. Everall (1973) The thickness of the epidermis. *Brit. J.*
7 *Dermatol.* **89**, 467-476.
- 8 18. Star, W. M. (1997) Light dosimetry in vivo. *Phys. Med. Biol.* **42**, 763-787.
- 9 19. Van Gemert, M. J. C., S. L. Jacques, H. J. C. M. Sterenborg, and W. M. Star (1989)
10 Skin optics. *IEEE Trans. Biomed. Eng.* **36**, 1146-1154.
- 11 20. Salomatina, E., B. Jiang, J. Novak, and A. N. Yaroslavsky (2006) Optical properties of
12 normal and cancerous human skin in the visible and near-infrared spectral range. *J.*
13 *Biomed. Opt.* **11**.
- 14 21. Young, A. R. (1997) Chromophores in human skin. *Phys. Med. Biol.* **42**, 789-802.
- 15 22. Alaluf, S., D. Atkins, K. Barrett, M. Blount, N. Carter, and A. Heath (2002) Ethnic
16 variation in melanin content and composition in photoexposed and photoprotected
17 human skin. *Pigment Cell Res.* **15**, 112-118.
- 18 23. Ito, S. and K. Wakamatsu (2003) Quantitative analysis of eumelanin and pheomelanin
19 in humans, mice, and other animals: A comparative review. *Pigment Cell Res.* **16**, 523-
20 531.

- 1 24. Del Bino, S., J. Sok, E. Bessac, and F. Bernerd (2006) Relationship between skin
2 response to ultraviolet exposure and skin color type. *Pigment Cell Res.* **19**, 606-614.
- 3 25. Taylor, S. C. (2002) Skin of color: Biology, structure, function, and implications for
4 dermatologic disease. *J. Am. Acad. Dermatol.* **46**, S41-S62.
- 5 26. Toda, K., M. A. Pathak, J. A. Parrish, T. B. Fitzpatrick, and W. C. Quevedo Jr (1972)
6 Alteration of racial differences in melanosome distribution in human epidermis after
7 exposure to ultraviolet light. *Nat. New. Biol.* **236**, 143-145.
- 8 27. Olson, R. L., J. Gaylor, and M. A. Everett (1973) Skin color, melanin, and erythema.
9 *Arch. Dermatol.* **108**, 541-544.
- 10 28. Irwin, C., A. Barnes, D. Veres, and K. Kaidbey (1993) An ultraviolet radiation action
11 spectrum for immediate pigment darkening. *Photochem. Photobiol.* **57**, 504-507.
- 12 29. Pathak, M. A., F. C. RILEY, and T. B. Fitzpatrick (1962) Melanogenesis in human skin
13 following exposure to long-wave ultraviolet and visible light. *J. Invest. Dermatol.* **39**,
14 435-443.
- 15 30. Lavker, R. M. and K. H. Kaidbey (1982) Redistribution of melanosomal complexes
16 within keratinocytes following UV-A irradiation: A possible mechanism for cutaneous
17 darkening in man. *Arch. Dermatol. Res.* **272**, 215-228.

18

19

20

21

1 **TABLES**

2 Table 1 Volume fractions of melanosomes used to represent the difference skin types (14)

| Skin type | Melanosome volume fraction |
|------------------|-----------------------------------|
| Very fair | 0.0255 |
| Light | 0.0865 |
| Dark | 0.305 |

3

For Peer Review

- 1 Table 2 Thickness (d) in mm, anisotropy (g) and refractive index (n) of the different skin
- 2 layers used

| Skin layer | Anisotropy (g) | Refractive index (n) | Thickness (d) (mm) |
|-------------------|------------------------------------|--|--|
| Stratum corneum | 0.9 | 1.53 | 0.015 |
| Epidermis | 0.79 | 1.5 | 0.038, 0.0875 |
| Dermis | 0.82 | 1.4 | 1.8 |

3

For Peer Review

1 **FIGURE CAPTIONS**

2

3 **Figure 1.** The Realistic Skin Model (RSM) showing the Stratum corneum, epidermal and
4 dermal skin layers as well as the excitation laser beam (Gaussian profile and beam diameter
5 of 0.4 mm). The red spots on the model boundaries are the photons leaving the model.

6

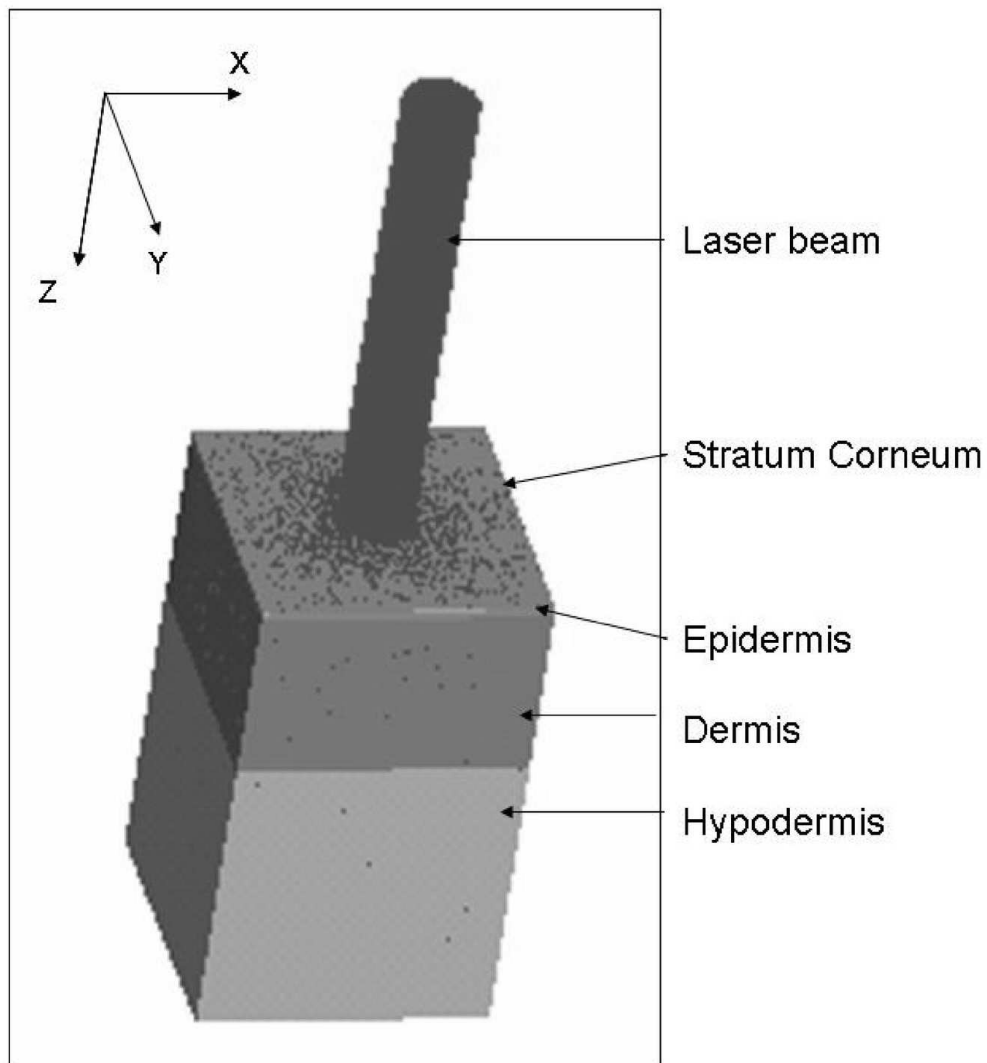
7 **Figure 2.** Absorbance spectra (attenuation coefficient as a function of wavelength) of
8 synthetic eumelanin samples for different concentrations at pH ~7.01.

9

10 **Figure 3.** Comparison of absorbance spectra of skin-like phantoms containing (a) 3 μ L
11 Intralipid and (b) 30 μ L Intralipid. Phantoms are also compared to the melanin only samples
12 of same concentrations from Fig. 2.

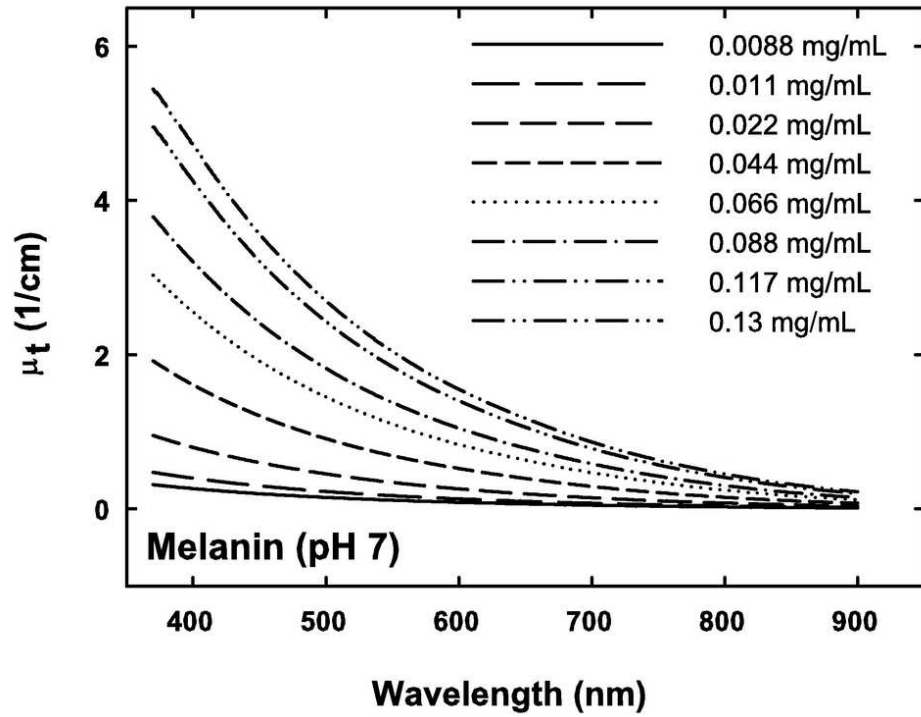
13

14 **Figure 4.** Comparison of the cumulative absorbed power (mW) as a function of wavelength
15 for epidermal thicknesses (ET) of (a) 38 μ m and (b) 87.5 μ m up to a skin depth of 0.12 mm.



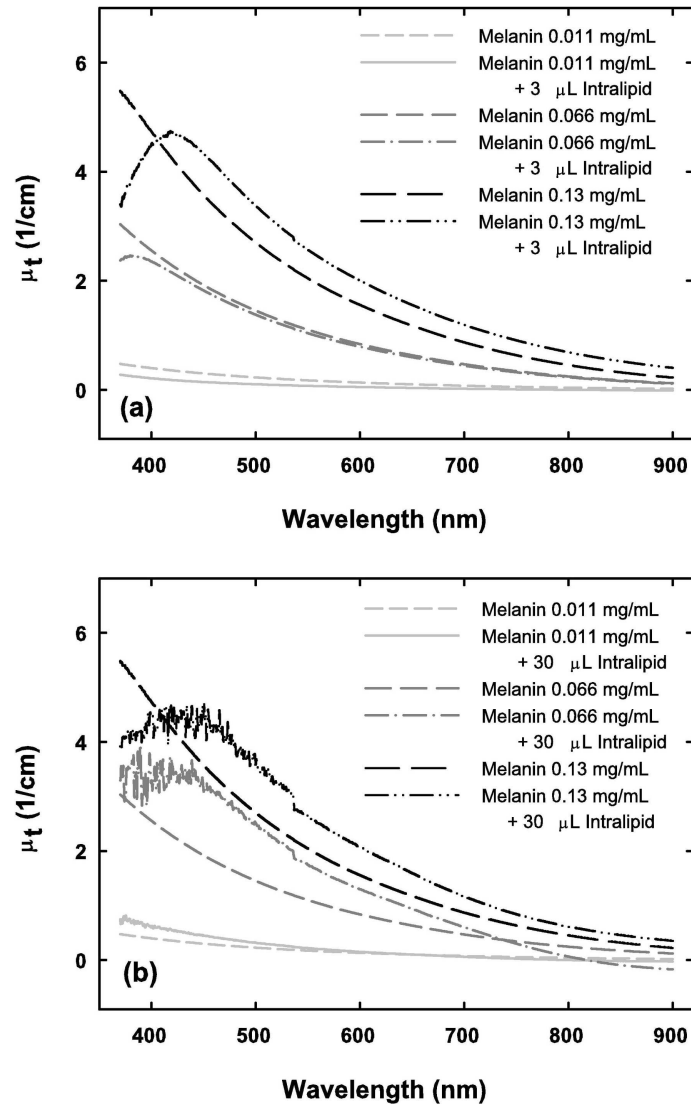
The Realistic Skin Model (RSM) showing the Stratum corneum, epidermal and dermal skin layers as well as the excitation laser beam (Gaussian profile and beam diameter of 0.4 mm). The red spots on the model boundaries are the photons leaving the model.

113x123mm (300 x 300 DPI)



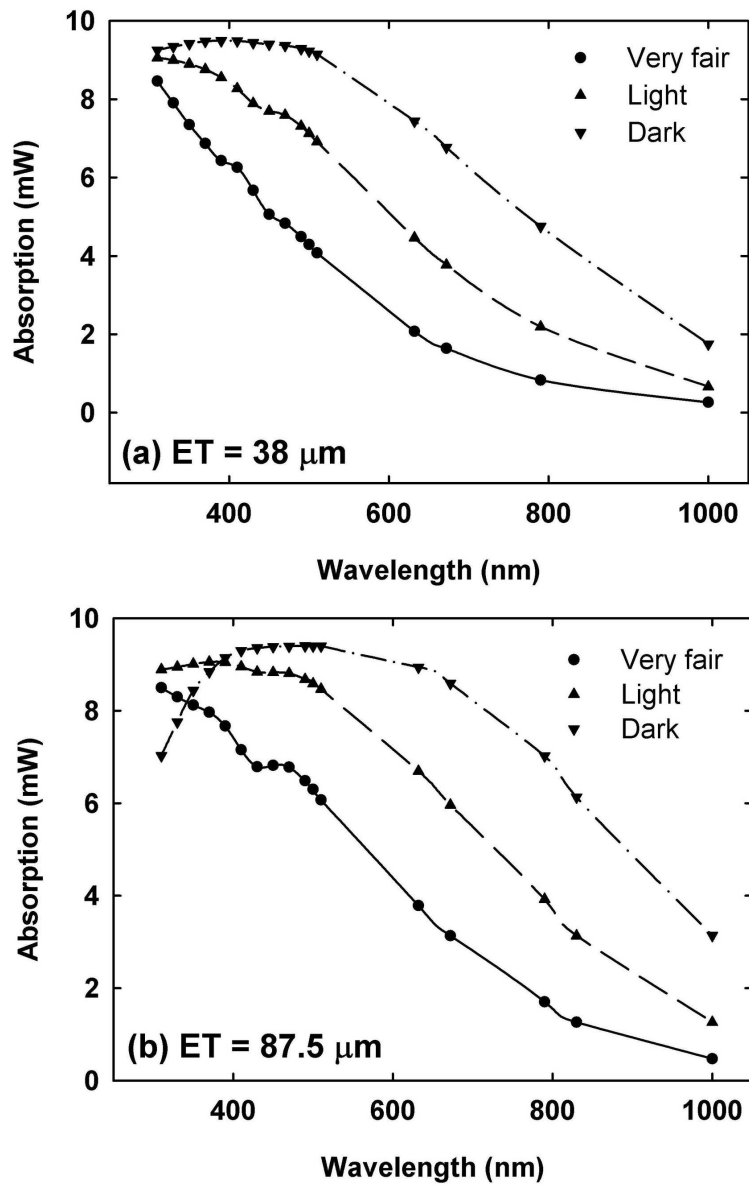
Absorbance spectra (attenuation coefficient as a function of wavelength) of synthetic eumelanin samples for different concentrations at pH \sim 7.01.
86x73mm (300 x 300 DPI)

iew



Comparison of absorbance spectra of skin-like phantoms containing (a) 3 μL Intralipid and (b) 30 μL Intralipid. Phantoms are also compared to the melanin only samples of same concentrations from Fig. 2.

163x263mm (300 x 300 DPI)



Comparison of the cumulative absorbed power (mW) as a function of wavelength for epidermal thicknesses (ET) of (a) 38 μm and (b) 87.5 μm up to a skin depth of 0.12 mm.
152x228mm (300 x 300 DPI)